Joule Heating Effect on Field-Free Magnetization Switching by Spin-Orbit Torque in Exchange-Biased Systems

Seyed Armin Razavi, Di Wu, Guoqiang Yu, Yong-Chang Lau, Kin L. Wong, Weihua Zhu, Congli He, Zongzhi Zhang, J. M. D. Coey, Plamen Stamenov, Pedram Khalili Amiri, and Kang L. Wang

Phys. Rev. Applied **7**, 024023 — Published 23 February 2017

DOI: 10.1103/PhysRevApplied.7.024023

Joule heating effect on field-free magnetization switching by spin-orbit torque in exchange-biased systems

Seyed Armin Razavi,[1*] Di Wu,[1,2*] Guoqiang Yu,[1†] Yong-Chang Lau,[3] Kin L. Wong,[1] Weihua Zhu,[2] Congli He,[1] Zongzhi Zhang,[2] J. M. D. Coey,[3] Plamen Stamenov,[3] Pedram Khalili Amiri,[1,4] Kang L. Wang[1]

[1]*Department of Electrical Engineering, University of California, Los Angeles, California 90095-1594, USA*
[2]*Key Laboratory of Micro and Nano Photonic Structures (Ministry of Education), Department of Optical Science and Engineering, Fudan University, Shanghai 200433, China*
[3]*CRANN, AMBER and School of Physics, Trinity College Dublin, Dublin 2, Ireland*
[4]*Inston Inc., Los Angeles, California 90095, USA*

[*]*These two authors contributed equally to this work.*
[†]*Corresponding author: guoqiangyu@ucla.edu*

Abstract

Switching of magnetization via spin-orbit torque provides an efficient alternative for non-volatile memory and logic devices. However, to achieve deterministic switching of perpendicular magnetization, an external magnetic field collinear with the current is usually required, which makes these devices inappropriate for practical applications. In this work, we examine the current-induced magnetization switching in a perpendicularly magnetized exchange-biased Pt/CoFe/IrMn system. An unconventional magnetic field annealing technique is used to introduce in-plane exchange biases, which are quantitatively characterized. Under proper conditions, field-free current-driven switching is achieved. We study Joule heating effect, and we show how it can decrease the in-plane exchange bias, and degrade the field-free switching. Furthermore, we discuss that the exchange bias training effect can have similar effects.

I. Introduction

Spin-orbit torque (SOT) switching of magnetization is a promising emerging technology for memory and logic applications [1-3], which offers an advantage over conventional spin transfer torque (STT) in terms of dynamic power dissipation [4-6]. However, to achieve high bit densities perpendicular magnetization is required [7]. Switching of perpendicular magnetization by SOT has been widely investigated; when an in-plane charge current is passed through a material with high spin-orbit coupling, such as a heavy metal layer (Pt [1,3,8], Ta [9-11], W [12], and Hf [13,14]), or even a topological insulator [15], a spin current is generated and it can apply torques on the adjacent ferromagnetic layer [3,8,16-18]. However, deterministic switching of perpendicular magnetization, driven by SOT requires an additional inversion symmetry breaking [19]. Usually, this has been achieved by applying an external magnetic field collinear with current, which is impractical in device applications.

There have been efforts to achieve deterministic switching without the need of an external field. Field-free switching has been achieved by introducing a lateral structural asymmetry, where the thickness of one layer is changed laterally [10,19,20], or by inducing a tilt in the uniaxial anisotropy axis [21]. More recently, field-free switching was realized in the antiferromagnet/ferromagnet systems, where some form of in-plane exchange bias (EB) is used instead of an external field [22-25].

In this work, we use an unconventional technique for magnetic field annealing, based on current-induced Joule heating, and a method for in-plane EB characterization

based on measurement of the anomalous Hall effect. With the help of these techniques, we study the field-free switching in the exchange biased films with the core structure of Pt/CoFe/IrMn. The in-plane EB at the interface of CoFe and IrMn replaces the external field and leads to deterministic field-free switching. By examining the in-plane EB on the device level, we characterize the Joule heating and EB training effects in these structures. We discuss how these effects reduce the in-plane EB field over several switching cycles, and hence, degrade the field-free switching. The results may find potential applications in SOT devices.

II. Sample Preparation and Magnetic Characterizations

The samples consisting of Ta(2)/Pt(3)/CoFe(0.9; 1.1)/IrMn(3)/Pt(1) (thicknesses in nm) were grown on Si/SiO_2 substrates by DC magnetron sputtering at room temperature. The samples were patterned into an array of Hall bar devices by standard photolithography and dry etching techniques. The Hall bars have dimensions of $20\mu m \times 130\mu m$ and $10\mu m \times 40\mu m$. These devices were measured using a Keithley 6221 current source, a Keithley 2182A nano-voltmeter and a Stanford Research Systems SR830 lock-in amplifier. For low temperature measurements physical properties measurement system (PPMS) was used. The external magnetic field was generated by an electromagnet, driven by a Kepco power supply. All measurements were carried out at room temperature, unless specified. All the magnetic characterizations were done on the device level, in order to be more consistent with the rest of the results. The resistance characterizations were carried out

using four-probe measurements. Similar results were also obtained in several batches of the same structures.

The current-driven field-free switching mechanism is depicted in Fig. 1(a). A charge current passing through Pt generates a spin current via the spin Hall effect, and the resulting spin current exerts torques on the magnetization of the CoFe layer. The schematic of the measurement is depicted in Fig. 1(b). The magnetic properties characterized by anomalous Hall measurement are shown in Fig. 2. Here, the samples were annealed with an out-of-plane magnetic field of 1 T for 10 minutes, in the $-Z$-direction. Figures 2(a) and 2(b) show anomalous Hall resistance as a function of out-of-plane and in-plane magnetic fields, respectively. In Fig. 2(a) the difference between the resistances of two states is defined by ΔR_{field}, which represents the total change in perpendicular magnetization, measured by anomalous Hall effect, when an out-of-plane external magnetic field is used to switch the magnetization. Perpendicular magnetic anisotropy and out-of-plane EB is present in both samples. The small hysteresis loops in Fig. 2(b) may be a result of misalignment between the external in-plane field and the film's surface. It should also be noted that because of the EB in Fig. 2(b), the samples do not switch between the two stable states along the easy-axis, only one of the up or down states is observed. As expected, the sample with $t_{CoFe} = 0.9$ nm has a larger EB, because of its thinner ferromagnetic layer [26]. However, the sample with $t_{CoFe} = 1.1$ nm switches at lower critical current densities, which should be more appropriate for field-free switching, since the Joule heating effects are relatively smaller. We also tried CoFe layers thinner than 0.9 nm, but as

expected, they have even larger critical switching currents, and consequently, a more pronounced Joule heating effect. Furthermore, samples with CoFe layers thicker than 1.1 nm do not have a good perpendicular magnetic anisotropy and are not useful for the applications. As will be discussed in section V, the Joule heating effects were found to degrade the field-free switching; hence, for all the switching measurements we used the sample with $t_{CoFe} = 1.1$ nm.

III. Current Driven Magnetization Switching with Out-of-Plane Exchange Bias

We first discuss the current-driven switching in the presence of an out-of-plane EB, to show the possibility of switching by SOT, and to show that out-of-plane EB does not result in field-free switching. A harmonic technique is used to investigate the current-induced SOTs in this case [16,18,27]. It should be noted that in this device, $\xi \equiv \Delta R_P / \Delta R_A = 0.12$, which is the ratio between the planar Hall effect and anomalous Hall effect resistances. To measure ΔR_P (planar Hall effect resistance), a large in-plane field of 1.5 T was applied to the sample to make the magnetization in-plane. Then, the transverse resistance was measured as a function of the angle between the in-plane field and the current direction. ΔR_P is defined as the difference between the maximum and the minimum values of the transverse resistance. Furthermore, ΔR_A (anomalous Hall resistance) is defined in the same way as ΔR_{field}, shown in Fig. 2(a). For the harmonic measurements, a small AC current is passed through the current channel, in the presence of an in-plane magnetic field, applied

along current (voltage) channel for measuring damping-like (field-like) fields. The ratios corresponding to damping-like (B_L) and field-like (B_T) torques are then calculated, [27]

$$B_{L(T)} = -2\left(\frac{\partial V_{2\omega}}{\partial H_{L(T)}}\right)/\left(\frac{\partial^2 V_{\omega}}{\partial H_{L(T)}^2}\right), \quad (1)$$

where V_{ω} and $V_{2\omega}$ are the first and second harmonic anomalous Hall voltage signals, respectively. Figures 3(a)-(d) show the results for the first and second harmonic measurements, which are fitted by parabolic and linear functions, respectively. Finally, we can obtain the damping-like (ΔH_L) and field-like (ΔH_T) fields, [27]

$$\Delta H_L = (B_L \pm 2\xi B_T)/(1 - 4\xi^2),$$

$$\Delta H_T = (B_T \pm 2\xi B_L)/(1 - 4\xi^2), \quad (2)$$

where due to our measurement configuration, we use the positive sign in the numerator. Figure 3(e) shows the field-like and damping-like fields, at different peak currents. In the small current regime, the effective fields have a linear dependence on the applied current. Based on the resistances of each layer, the portion of current flowing through the Pt layer was calculated. We estimate that about 47% of the total current passes through the Pt layer. Therefore, the effective damping-like and field-like field efficiencies ($\Delta H_{L(T)}/J$) are calculated to be 22.31 and 7.04 Oe per 10^7 A/(cm)^2, respectively, where J is the peak current density passing through Pt. These values are slightly smaller than other reported values [28,29]. This can be due to the fact that a much smaller portion of the current passes through the IrMn layer, which also generates SOT, and its torques tend to partially cancel the torques from the Pt layer, since they have the same sign of spin Hall angle [30]. It should be noted that the

SOT responsible for switching stems from the Pt layer, rather than IrMn, because of its much higher current density. Assuming that the damping-like torque is a result of spin Hall effect solely, we can find the spin Hall angle using $\theta_{SHE} = \frac{-2|e|M_s t_F}{h} \times \frac{\Delta H_L}{J}$, where $|e|$, h, t_F, and M_s represent the absolute value of the electron's charge, Planck's constant, ferromagnetic layer thickness, and the saturation magnetization of the ferromagnetic layer [31]. Using SQUID measurement, the saturation magnetization was found to be 1100 emu/cm^3. The obtained spin Hall angle for Pt in this structure is 0.082, which is similar to the other reported values for Pt [32].

In order to achieve deterministic switching, we need to break the inversion symmetry, thus, as expected, the out-of-plane EB does not result in field-free switching. Anomalous Hall resistance is used for current-driven switching characterization, and the measurement setup is depicted in Fig. 1(b). For the switching measurement, first an initialization current pulse of +60 mA was applied to the sample. Then, the applied current was swept from +60 mA to −70 mA, and back to +60 mA, in the presence of different in-plane magnetic fields, which were collinear with the current direction. To make the switching measurements consistent with the other switching measurements in this work, pulses with 200 μs widths and a one-second wait between successive pulses were used to drive the magnetization switching.

The resulting plots are shown in Fig. 4. The anomalous Hall resistance is proportional to the perpendicular magnetization, thus, in order to better describe the current-driven switching under different in-plane magnetic fields, we look at the total change in anomalous Hall resistance after sweeping the current. ΔR_{field} ($\Delta R_{current}$) represents

the total perpendicular magnetization reversal when an out-of-plane field (current) is swept. In this case, $\Delta R_{field} = 0.473\ \Omega$. As can be seen in Fig. 4(a), $\Delta R_{current}$ is almost negligible for the zero field case, which indeed shows that there is no field-free switching. Applying negative and positive in-plane fields results in different switching polarities because of the opposite SOT directions [3]; however, $|\Delta R_{current}|$ is symmetric around the zero field. This shows that there is no shift in the switching diagram, which is reasonable since the EB direction is out-of-plane. The switching diagram is plotted in Fig. 4(b). The vertical axis shows $\Delta R_{current}/\Delta R_{field}$, which is plotted as a function of different external in-plane magnetic fields, H_L. $\Delta R_{current}/\Delta R_{field}$ represents the switching percentage of the sample's area as a result of applying current, detected by anomalous Hall effect. In our notations $\Delta R_{current}$ has a positive (negative) value if at large positive currents, the state with positive (negative) anomalous Hall resistance is preferred. Thus, positive and negative values of $\Delta R_{current}$ correspond to different switching polarities. In this case we do not have field-free switching; the very small shift in the switching diagram is negligible and may be due to the remanent in-plane field of the magnet.

As can be seen in Fig. 4(b), $\Delta R_{current}$ does not reach $0.473\ \Omega$, even in the presence of larger in-plane magnetic fields. We suppose this is due to the fact that the current density becomes smaller on the Hall bar cross section area, and does not reach the critical value. Furthermore, the additional pinning effect at the cross section area may make complete switching difficult [30]. Hence, the cross section region of the device is not completely switched, and $\Delta R_{current}$ does not reach ΔR_{field}.

IV. Field-Free Magnetization Switching with In-Plane Exchange Bias

A. In-Plane Exchange Bias Measurement

For field-free perpendicular magnetization switching, an in-plane EB needs to be introduced. For this purpose, the sample's temperature should be raised above the blocking temperature in the presence of a large in-plane magnetic field. The blocking temperature is defined as the lowest temperature at which the exchange bias becomes zero [26]. In order to extract the blocking temperature quantitatively, we measured the temperature-dependence of the out-of-plane EB. First, the sample was annealed with an out-of-plane field. Then, its temperature was reduced to 100 K in vacuum and in the presence of an out-of-plane field of 1 T. Subsequently, the out-of-plane EB was measured at different temperatures, up to 350 K, and by fitting the data the blocking temperature was found to be around 360 K.

We annealed the devices using current-induced Joule heating in the presence of a large in-plane magnetic field, which can saturate the magnetization. In this technique, a DC current with proper amplitude is applied to the device, which is placed inside a magnetic field. The amplitude of the applied current is large enough to raise the sample's temperature above the blocking temperature, but not to burn the device. The appropriate amplitude was found experimentally for each CoFe thickness. The magnetic field was applied along the longitudinal direction of the Hall bar; hence, the longitudinal EB was obtained, in the L-direction as shown in Fig. 1(b). For the sample with $t_{CoFe} = 1.1$ nm, we applied 20 mA and 30 mA DC currents, for the

10 μm and 20 μm Hall bar widths, respectively, which translates to a temperature of 400 K, according to the temperature-dependence of the resistance in the sample. This temperature is indeed higher than the blocking temperature. This amplitude resulted in the largest in-plane EB without damaging the structure. The current was applied for 10 minutes in the presence of an external field of 1.5 T. Then the samples were cooled for 5 minutes in the air with the magnetic field on. The samples had the same total resistance change ΔR_{field}, measured by anomalous Hall effect, after this procedure, which suggests that the magnetic properties are not degraded.

In order to measure the in-plane EB field, the anomalous Hall resistance was measured as a function of in-plane external field. The total magnetic energy can be expressed as

$$E = (-K_u + 2\pi M_s^2)\cos^2\theta - M_s(H_T\cos\varphi\sin\theta + H_L\sin\varphi\sin\theta + H_z\cos\theta), \quad (3)$$

where K_u is the magnetic anisotropy, which is in out-of-plane direction, M_s is the saturation magnetization, θ and φ are the polar and azimuthal angles of the magnetization, respectively, and H_T, H_L, and H_z are the transverse, longitudinal, and perpendicular magnetic field components, respectively, as illustrated in Fig. 1(b). It should be noted that here we are assuming that the magnetization remains uniform in the process. For in-plane EB measurement, an external field in the longitudinal direction was applied; hence $\varphi = 90°$. Thus, Eq. (3) can be rewritten as

$$E = (-K_u + 2\pi M_s^2)\cos^2\theta - M_s H_L'\sin\theta, \quad (4)$$

where $H_L' = H_L + H_{EB}^{IP}$ should be used instead of H_L, to account for the in-plane EB field. Here, we have assumed that the out-of-plane EB is small and negligible, which

can be confirmed by the out-of-plane AHE loop. For different values of external magnetic field, the total energy should be minimized with respect to θ, as a result

$$\frac{\partial E}{\partial \theta} = (-K_u + 2\pi M_s^2)(-\sin 2\theta) - M_s H_L' \cos\theta = 0. \quad (5)$$

Since H_L' is small compared to the anisotropy field, then $\cos\theta = 0$ is not a physically valid solution. Thus,

$$\sin\theta = \frac{M_s H_L'}{2(K_u - 2\pi M_s^2)} = \alpha H_L', \quad (6)$$

where $\alpha H_L'$ is very small, and α is a constant for each sample. The anomalous Hall resistance is proportional to the out-of-plane component of the magnetization, or $R_H \propto M_z = M\cos\theta = M\sqrt{1-(\alpha H_L')^2}$, which can be approximated near $\alpha H_L' = 0$ as $R_H \propto M\left(1 - \frac{\alpha^2 {H_L'}^2}{2}\right) = M(1 - \frac{\alpha^2}{2}(H_L + H_{EB}^{IP})^2)$. Consequently, in order to find the EB field, R_H is measured at multiple in-plane magnetic fields around its extremum, then a quadratic function is fitted, and the extremum value is found. The extremum is where $H_L' = H_L + H_{EB}^{IP} = 0$, so the EB field can be extracted. This is illustrated in Figs. 5(a) and 5(b). On the same structure as in section III ($t_{CoFe} =$ 1.1 nm) an in-plane EB field was introduced in two opposite directions, $\pm\hat{L}$. A small current of 0.5 mA amplitude was used to measure the anomalous Hall resistance, and the EB fields were extracted using the method described above. In this measurement, the in-plane magnetic field was swept back and forth, and each point on the graph represents the average of the two values. The difference of the EB magnitudes for the opposite directions comes from the fact that they are measured on two different devices. However, these devices both have the same structure and are from the same film; thus, this small difference does not affect the validity of the arguments.

This method enables us to quantitatively measure the in-plane EB at different stages in the process. Hence, we were able to do a comprehensive study on the Joule heating and training effects on the in-plane EB and field-free switching. These will be discussed in more detail in section V.

B. Field-Free Magnetization Switching

After obtaining large in-plane EB fields, field-free current-driven magnetization switching was achieved, as described in the following. The measurement is done as described in section III. Again, for these measurements a pulsed current is used. The results are depicted in Figs. 5(c) and 5(d), where field-free switching is observed as expected. The field-field switching polarity with positive (negative) EB field is the same as that with positive (negative) external in-plane field, which indicates that the in-plane EB indeed plays the role of the external field. Unlike Fig. 4(a), in this case $|\Delta R_{current}|$ is asymmetric with respect to different in-plane magnetic fields, H_L. We attribute this phenomenon to the presence of in-plane EB. Switching diagrams are plotted in Figs. 5(e), and 5(f). A clear shift in two different directions is observed, which is consistent with the EB field directions for each case. As a result of these shifts, field-free switching is achieved. This can be described very well with the depicted switching diagrams; in these cases, $\Delta R_{current}$ is large at zero field, but vanishes at some other in-plane field, where the EB cancels the external field, and no switching is observed. In these switching diagrams, $\Delta R_{current}/\Delta R_{field}$ at zero field are around 50% and 90% of the maximum values, respectively. The maximum value

of 0.81 is obtained for approximately 400 Oe in-plane field.

It should be noted that in both cases, the shift in the switching diagram is smaller than the measured in-plane EB field. As will be discussed in more detail in section V, this can be a result of the non-uniformity of the EB field throughout the device [22], or the in-plane EB reduction because of Joule heating or EB training effect [33]. However, this needs further investigation. Furthermore, the amount of shift in Figs. 5(e) and 5(f) is not the same. This may be due to Joule heating or EB training effect, which can change the in-plane EB during the measurement and consequently the observed shifts in the switching diagrams depend on the sequence in which the measurement was carried out.

V. Joule Heating and Exchange Bias Training Effects on the Field-Free Switching

A. Joule Heating Effect

In order to limit the heating effects in the current driven switching measurements, a pulsed current was used. The critical current for switching was around 40-50 mA, depending on the device dimensions, which translates to a current density of $\sim 4 \times 10^7$ A/cm^2 passing through the Pt layer. These relatively large amplitudes can increase the sample's temperature through Joule heating. The IrMn thickness of the structure used in the measurements is 3 nm; thus, a low blocking temperature is expected [34].

For a quantitative study of the Joule heating effects, we measured how the

temperature of the sample changes in the switching measurement. To that end, we measured how the resistance of the sample changes during the time that the pulses are applied for switching. We also measured the temperature-dependence of resistance, in a range from 110 K to 350 K, and we extrapolated the resistance at higher temperatures. By comparing these two sets of data we were able to estimate the temperature changes during switching. As can be seen in Fig. 6(a), the temperature can rise up to 500 K during the switching, which is well above the blocking temperature. This can result in an irreversible loss of the exchange bias.

In order to show the importance of heating effects in these structures, we compare the field-free switching of a sample under pulsed and DC currents. For the DC current measurement, which is an extreme case in terms of Joule heating, the amplitude of the applied current changes from large negative values to large positive values, and back, with no delay between consecutive values. Each value is applied for around 200 ms. For this purpose, a sample with $t_{CoFe} = 1.1$ nm was annealed using the current. An in-plane EB field of 540 Oe was introduced in the sample. Then the sample was switched using DC current at zero external field. Afterwards, the annealing procedure was repeated to ensure that the in-plane EB field of 540 Oe is still present. This time the sample was switched at zero external field using pulsed current. The results are shown in Fig. 6(b). With pulsed current, field-free switching is achieved, while with DC current almost no change in Hall resistance (or equivalently in perpendicular magnetization) is observed. We attribute this effect to Joule heating, and its impact on the disappearance of the in-plane EB, since the temperature of the sample rises above

the blocking temperature during the measurement.

Furthermore, even if pulsed current is used, the field-free switching still degrades after repeating the measurement several times. This can be seen in Fig. 6(c). Here, the field-free switching measurement, of the same structure used above, is repeated 12 times. The total change in Hall resistance in the switching measurement is decreased, and the field-free switching is disappearing over the time. This can again be attributed to the Joule heating effect. However, in this case the EB training effect may also be a contributing factor, and this will be discussed in the next section.

With the help of our device-level in-plane EB measurement technique, it was observed that after each current-driven field-free switching cycle, the in-plane EB was reduced, and eventually it disappeared, as depicted in Fig. 7(a). As noted, in the switching measurement, the temperature of the sample goes above the blocking temperature during the pulse application time. On the other hand, the relevant timescale τ for antiferromagnetic re-ordering is given by [22,35]

$$\frac{1}{\tau} = \nu_0 \exp\left(-\frac{E_b}{k_B T}\right), \quad (7)$$

where $\nu_0 \approx 10^9$ Hz is the attempt frequency, E_b is the energy barrier for antiferromagnetic grain reversal, k_B is the Boltzmann's constant, and T is the temperature. For samples with several weeks of stability, τ is around 10^6 s at room temperature (T_0), which results in $E_b \approx 34.5 \times k_B T_0$. The temperature in our measurement goes as high as 500 K, so the corresponding timescale τ would be ~1 s, which is much longer than the pulse duration of 200 μs. Consequently, the exchange bias does not vanish with one large pulse; it decreases gradually after many pulses.

This can also explain why in the DC measurement no field-free switching is observed. In the DC measurement the high temperature is kept for much longer than 1 s; as a result, the exchange bias vanishes instantly and no field-free switching is observed. It should be noted that the Joule heating of the 0.1 mA current, used for in-plane EB measurement, was found to be negligible, based on a control measurement in which only the current was applied. In the control measurement, the sample was not switched; only an in-plane field was applied to measure the in-plane EB successively, and after 20 times there was no significant change in the EB value. This shows that the heating effect of the 0.1 mA current can be neglected.

The disappearance of in-plane EB as a result of heating can be further supported by the comparison of anomalous Hall data, R_H as a function of H_z, at different stages in the process: before and after current annealing with in-plane field, and after current-driven switching measurement, shown in Fig. 7(b). After annealing in the presence of a large in-plane magnetic field, the out-of-plane EB decreases, which shows that the pinning is in the in-plane direction. Also, the coercivity is decreased by ~100 Oe when the out-of-plane EB decreases, which agrees with other reported findings [36]. After annealing, current was used to switch the sample through twelve cycles, where the critical current for switching was around 45 mA. After current-driven switching measurement, the out-of-plane EB appears again, this time in the form of double loops. This further indicates the presence of heating effects. The temperature of the sample, with perpendicular easy axis, is raised above the blocking temperature in the course of switching measurement, in the absence of any large

external fields. Consequently, the out-of-plane EB tends to appear again, but there is no preference between upward and downward pinning directions, because both are along the easy axis and there is no external field to make a preference. Thus, some parts of the sample have an upward and the other parts have a downward pinning, hence the double loop EB appears.

Increasing the IrMn thickness raises the Néel and blocking temperatures; however, that is not desirable since it will also increase the shunting effect. The SOT for switching stems from the Pt layer, as shown in section III. By increasing the IrMn thickness, the shunting effect becomes significant and less current passes through Pt. Consequently, the critical current for switching increases. This will result in more Joule heating effect and is not desirable. We tried samples with thicker IrMn layers up to 10 nm, but field-free switching was not achieved in them.

The Joule heating effect is helpful when switching is assisted with an external in-plane field. In the same sample, using DC current reduces the critical current density for switching by 10% compared to the case where pulsed current is used. That is due to the fact that Joule heating effect raises the temperature of the sample and reduces the anisotropy, and consequently switching becomes easier. On the other hand, when an in-plane EB is used for field-free switching, the heating effect is no longer desirable, since it reduces the in-plane EB field. In this case avoiding the thermal effect is crucial.

B. Exchange Bias Training Effect

Even if very short pulses with negligible heating effects are used, the in-plane EB will

not be constant after successive switchings, due to the EB training effect. The training has mostly been investigated in cases where an external magnetic field is used for cycling through hysteresis loops [33,37,38]. However, it can also exist when SOT is used for magnetization switching. The spin structure at the interface of AFM/FM deviates from its equilibrium state when an EB field is created. Consecutive switchings can result in a rearrangement of the IrMn's spin structure at the interface of IrMn/CoFe towards an equilibrium state [33]. Consequently, a gradual decrease in the in-plane EB is possible. It should be noted that there are also some other models and explanations provided for the origin of EB training effect [38-43]. However, in this work we only focus on the general concept.

In order to show this effect in our structure, a sample with $t_{CoFe} = 1.1\,\mathrm{nm}$ was current annealed, and an in-plane EB field of $560\,\mathrm{Oe}$ was introduced. Then an out-of-plane external field was used to switch the sample back and forth. Afterwards, the in-plane EB was measured again and so on. The result is depicted in Fig. 8. After each out-of-plane loop, the in-plane EB is decreased, and this can be attributed to training effect. In our case, SOT is used to switch the perpendicular magnetization. However, as described above, multiple switchings of the magnetization, itself, result in a reduction of the in-plane EB. This can be a major problem for these devices, since the in-plane EB is essential for field-free switching. As shown in Fig. 8, after only 20 successive switchings, the in-plane EB is reduced by around 30%. This effect will deteriorate the device performance very fast over the time. By comparing the results of Fig. 7(a) and Fig. 8, it can be seen that in our measurements, the Joule heating

effect is dominant over the exchange bias training effect, in terms of decreasing the in-plane EB.

VI. Conclusion

Field-free perpendicular magnetization switching driven by spin-orbit torque in an asymmetric exchange-biased system of Ta/Pt/CoFe/IrMn/Pt was achieved with the help of device-level magnetic field annealing. The induced in-plane EB plays the role of the external magnetic field required for breaking system symmetry. Through in-plane EB characterization techniques, and a study of Joule heating and EB training effects, it is found that they can significantly affect the field-free switching in these structures. In order to make practical applications possible, these are very important issues that need to be addressed. To have more robust field-free switching, very narrow pulses can help with Joule heating problem, as suggested by the comparison of DC and pulsed currents for switching, where a significant improvement can be seen with pulsed currents. Furthermore, a thin layer inserted between the ferromagnetic and antiferromagnetic layers can help with thermal stability [22]. The training effect is known to be smaller in structures with single crystalline AFM layers [26], thus, that may potentially help with the training effect problem. Furthermore, as shown in Fig. 8, there is a saturation value for the in-plane EB, which can be high enough to be used for field-free switching. However, the training effect has to be studied in these devices, and they should be designed to have an adequate saturation value.

Acknowledgement

This work was supported in part by C-SPIN and FAME, two of six centers of STARnet, a Semiconductor Research Corporation program, sponsored by MARCO and DARPA. This work was also supported by the National Science Foundation (ECCS 1611570) and Nanosystems Engineering Research Center for Translational Applications of Nanoscale Multiferroic Systems (TANMS) Cooperative Agreement Award EEC-1160504. We would like to acknowledge the collaboration of this research with the King Abdul-Aziz City for Science and Technology (KACST) via The Center of Excellence for Green Nanotechnologies (CEGN). This work was supported as part of the SHINES Center, an Energy Frontier Research Center funded by the U.S. Department of Energy, Office of Science, Basic Energy Sciences under Award # S000686. D. Wu and Z. Z. Zhang thank the support of China Scholarship Council (CSC), the 973 Program (2014CB921104) and the National Natural Science Foundation of China (NSFC) grant (11474067). Y.-C. Lau, P. Stamenov and J. M. D. Coey acknowledge the support by Science Foundation Ireland through AMBER and by grant no. 13/ERC/I2561. In addition, G. Q. Y. acknowledges Junyang Chen for fruitful discussions.

[1] I. M. Miron, K. Garello, G. Gaudin, P. J. Zermatten, M. V. Costache, S. Auffret, S. Bandiera, B. Rodmacq, A. Schuhl, and P. Gambardella, Perpendicular switching of a single ferromagnetic layer induced by in-plane current injection, Nature **476**, 189 (2011).

[2] L. Liu, C. F. Pai, Y. Li, H. W. Tseng, D. C. Ralph, and R. A. Buhrman, Spin-Torque Switching with the Giant Spin Hall Effect of Tantalum, Science **336**, 555 (2012).

[3] L. Liu, O. J. Lee, T. J. Gudmundsen, D. C. Ralph, and R. A. Buhrman, Current-Induced Switching of Perpendicularly Magnetized Magnetic Layers Using Spin Torque from the Spin Hall Effect, Physical Review Letters **109**, 096602 (2012).

[4] R. Dorrance, J. G. Alzate, S. S. Cherepov, P. Upadhyaya, I. N. Krivorotov, J. A. Katine, J. Langer, K. L. Wang, P. K. Amiri, and D. Marković, Diode-MTJ Crossbar Memory Cell Using Voltage-Induced Unipolar Switching for High-Density MRAM, IEEE Electron Device Letters **34**, 753 (2013).

[5] K. L. Wang, J. G. Alzate, and P. K. Amiri, Low-power non-volatile spintronic memory: STT-RAM and beyond, Journal of Physics D: Applied Physics **46**, 7 (2013).

[6] S. Ikeda, K. Miura, H. Yamamoto, K. Mizunuma, H. D. Gan, M. Endo, S. Kanai, J. Hayakawa, F. Matsukura, and H. Ohno, A perpendicular-anisotropy CoFeB–MgO magnetic tunnel junction, Nature Materials **9**, 721 (2010).

[7] S. Mangin, D. Ravelosona, J. A. Katine, M. J. Carey, B. D. Terris, and E. E. Fullerton, Current-induced magnetization reversal in nanopillars with perpendicular anisotropy, Nature Materials **5**, 210 (2006).

[8] X. Qiu, K. Narayanapillai, Y. Wu, P. Deorani, D. H. Yang, W. S. Noh, J. H. Park, K. J. Lee, H. W. Lee, and H. Yang, Spin–orbit-torque engineering via oxygen manipulation, Nature Nanotechnology **10**, 333 (2015).

[9] C. Zhang, S. Fukami, H. Sato, F. Matsukura, and H. Ohno, Spin-orbit torque induced magnetization switching in nano-scale Ta/CoFeB/MgO, Applied Physics Letters **107**, 012401 (2015).

[10] G. Yu, L. T. Chang, M. Akyol, P. Upadhyaya, C. He, X. Li, K. L. Wong, P. K. Amiri, and K. L. Wang, Current-driven perpendicular magnetization switching in Ta/CoFeB/[TaOx or MgO/TaOx] films with lateral structural asymmetry, Applied Physics Letters **105**, 102411 (2014).

[11] C. O. Avci, K. Garello, C. Nistor, S. Godey, B. Ballesteros, A. Mugarza, A. Barla, M. Valvidares, E. Pellegrin, A. Ghosh, I. M. Miron, O. Boulle, S. Auffret, G. Gaudin, and P. Gambardella, Fieldlike and antidamping spin-orbit torques in as-grown and annealed Ta/CoFeB/MgO layers, Physical Review B **89**, 214419 (2014).

[12] C. F. Pai, L. Liu, Y. Li, H. W. Tseng, D. C. Ralph, and R. A. Buhrman, Spin transfer torque devices utilizing the giant spin Hall effect of tungsten, Applied Physics Letters **101**, 122404 (2012).

[13] M. Akyol, G. Yu, J. G. Alzate, P. Upadhyaya, X. Li, K. L. Wong, A. Ekicibil, P. K. Amiri, and K. L. Wang, Current-induced spin-orbit torque switching of perpendicularly magnetized Hf|CoFeB|MgO and Hf|CoFeB|TaOx structures, Applied Physics Letters **106**, 162409 (2015).

[14] M. Akyol, J. G. Alzate, G. Yu, P. Upadhyaya, K. L. Wong, A. Ekicibil, P. K. Amiri, and K. L. Wang, Effect of the oxide layer on current-induced spin-orbit torques in Hf|CoFeB|MgO and Hf|CoFeB|TaOx structures, Applied Physics Letters **106**, 032406 (2015).

[15] Y. Fan, P. Upadhyaya, X. Kou, M. Lang, S. Takei, Z. Wang, J. Tang, L. He, L. T. Chang, M. Montazeri, G. Yu, W. Jiang, T. Nie, R. N. Schwartz, Y. Tserkovnyak, and K. L. Wang, Magnetization switching through giant spin–orbit torque in a magnetically doped topological insulator heterostructure, Nature Materials **13**, 699 (2014).

[16] J. Kim, J. Sinha, M. Hayashi, M. Yamanouchi, S. Fukami, T. Suzuki, S. Mitani, and H. Ohno, Layer

thickness dependence of the current-induced effective field vector in Ta|CoFeB|MgO, Nature Materials **12**, 240 (2013).

[17] L. Liu, T. Moriyama, D. C. Ralph, and R. A. Buhrman, Spin-Torque Ferromagnetic Resonance Induced by the Spin Hall Effect, Physical Review Letters **106**, 036601 (2011).

[18] K. Garello, I. M. Miron, C. O. Avci, F. Freimuth, Y. Mokrousov, S. Blügel, S. Auffret, O. Boulle, G. Gaudin, and P. Gambardella, Symmetry and magnitude of spin–orbit torques in ferromagnetic heterostructures, Nature Nanotechnology **8**, 587 (2013).

[19] G. Yu, P. Upadhyaya, Y. Fan, J. G. Alzate, W. Jiang, K. L. Wong, S. Takei, S. A. Bender, L. T. Chang, Y. Jiang, M. Lang, J. Tang, Y. Wang, Y. Tserkovnyak, P. K. Amiri, and K. L. Wang, Switching of perpendicular magnetization by spin–orbit torques in the absence of external magnetic fields, Nature Nanotechnology **9**, 548 (2014).

[20] G. Yu, M. Akyol, P. Upadhyaya, X. Li, C. He, Y. Fan, M. Montazeri, J. G. Alzate, M. Lang, K. L. Wong, P. K. Amiri, and K. L. Wang, Competing effect of spin-orbit torque terms on perpendicular magnetization switching in structures with multiple inversion asymmetries, Scientific Reports **6**, 23956 (2016).

[21] J. Torrejon, F. Garcia-Sanchez, T. Taniguchi, J. Sinha, S. Mitani, J. V. Kim, and M. Hayashi, Current-driven asymmetric magnetization switching in perpendicularly magnetized CoFeB/MgO heterostructures, Physical Review B **91**, 214434 (2015).

[22] A. v. d. Brink, G. Vermijs, A. Solignac, J. Koo, J. T. Kohlhepp, H. J. M. Swagten, and B. Koopmans, Field-free magnetization reversal by spin-Hall effect and exchange bias, Nature Communications **7**, 10854 (2016).

[23] S. Fukami, C. Zhang, S. DuttaGupta, A. Kurenkov, and H. Ohno, Magnetization switching by spin–orbit torque in an antiferromagnet–ferromagnet bilayer system, Nature Materials **15**, 535 (2016).

[24] Y. C. Lau, D. Betto, K. Rode, J. M. D. Coey, and P. Stamenov, Spin–orbit torque switching without an external field using interlayer exchange coupling, Nature Nanotechnology **11**, 758 (2016).

[25] Y. W. Oh, S. C. Baek, Y. M. Kim, H. Y. Lee, K. D. Lee, C. G. Yang, E. S. Park, K. S. Lee, K. W. Kim, G. Go, J. R. Jeong, B. C. Min, H. W. Lee, K. J. Lee, and B. G. Park, Field-free switching of perpendicular magnetization through spin–orbit torque in antiferromagnet/ferromagnet/oxide structures, Nature Nanotechnology (2016).

[26] J. Nogués and I. K. Schuller, Exchange bias, Journal of Magnetism and Magnetic Materials **192**, 203 (1999).

[27] M. Hayashi, J. Kim, M. Yamanouchi, and H. Ohno, Quantitative characterization of the spin-orbit torque using harmonic Hall voltage measurements, Physical Review B **89**, 144425 (2014).

[28] M. Yang, K. Cai, H. Ju, K. W. Edmonds, G. Yang, S. Liu, B. Li, B. Zhang, Y. Sheng, S. Wang, Y. Ji, and K. Wanga, Spin-orbit torque in Pt/CoNiCo/Pt symmetric devices, Scientific Reports **6**, 20778 (2016).

[29] S. Emori, U. Bauer, S. Woo, and G. S. D. Beach, Large voltage-induced modification of spin-orbit torques in Pt/Co/GdOx, Applied Physics Letters **105**, 222401 (2014).

[30] D. Wu, G. Yu, C. T. Chen, S. A. Razavi, Q. Shao, X. Li, B. Zhao, K. L. Wong, C. He, Z. Zhang, P. K. Amiri, and K. L. Wang, Spin-orbit torques in perpendicularly magnetized Ir22Mn78/Co20Fe60B20/MgO multilayer, Applied Physics Letters **109**, 222401 (2016).

[31] G. Yu, P. Upadhyaya, K. L. Wong, W. Jiang, J. G. Alzate, J. Tang, P. K. Amiri, and K. L. Wang, Magnetization switching through spin-Hall-effect-induced chiral domain wall propagation, Physical Review B **89**, 104421 (2014).

[32] J.-C. Rojas-Sánchez, N. Reyren, P. Laczkowski, W. Savero, J.-P. Attané, C. Deranlot, M. Jamet, J.-M.

George, L. Vila, and H. Jaffrès, Spin Pumping and Inverse Spin Hall Effect in Platinum: The Essential Role of Spin-Memory Loss at Metallic Interfaces, Physical Review Letters **112**, 106602 (2014).
[33] C. Binek, Training of the exchange-bias effect: A simple analytic approach, Physical Review B **70**, 014421 (2004).
[34] M. Ali, C. H. Marrows, M. Al-Jawad, B. J. Hickey, A. Misra, U. Nowak, and K. D. Usadel, Antiferromagnetic layer thickness dependence of the IrMn/Co exchange-bias system, Physical Review B **68**, 214420 (2003).
[35] H. Xi and R. M. White, Theory of the blocking temperature in polycrystalline exchange biased bilayers based on a thermal fluctuation model, Journal of Applied Physics **94**, 5850 (2003).
[36] S. Maat, K. Takano, S. S. P. Parkin, and E. E. Fullerton, Perpendicular Exchange Bias of Co/Pt Multilayers, Physical Review Letters **87**, 087202 (2001).
[37] A. Hochstrat, C. Binek, and W. Kleemann, Training of the exchange-bias effect in NiO-Fe heterostructures, Physical Review B **66**, 092409 (2002).
[38] K. Zhang, T. Zhao, and H. Fujiwara, Training effect of exchange biased iron–oxide/ferromagnet systems, Journal of Applied Physics **89**, 6910 (2001).
[39] P. Miltényi, M. Gierlings, J. Keller, B. Beschoten, G. Güntherodt, U. Nowak, and K. D. Usadel, Diluted Antiferromagnets in Exchange Bias: Proof of the Domain State Model, Physical Review Letters **84**, 4224 (2000).
[40] T. Gredig, I. N. Krivorotov, and E. D. Dahlberg, Magnetization reversal in exchange biased Co/CoO probed with anisotropic magnetoresistance, Journal of Applied Physics **91**, 7760 (2002).
[41] F. Radu, M. Etzkorn, R. Siebrecht, T. Schmitte, K. Westerholt, and H. Zabel, Interfacial domain formation during magnetization reversal in exchange-biased CoO/Co bilayers, Physical Review B **67**, 134409 (2003).
[42] T. Hauet, J. A. Borchers, P. Mangin, Y. Henry, and S. Mangin, Training Effect in an Exchange Bias System: The Role of Interfacial Domain Walls, Physical Review Letters **96**, 067207 (2006).
[43] S. Brems, K. Temst, and C. V. Haesendonck, Origin of the Training Effect and Asymmetry of the Magnetization in Polycrystalline Exchange Bias Systems, Physical Review Letters **99**, 067201 (2007).

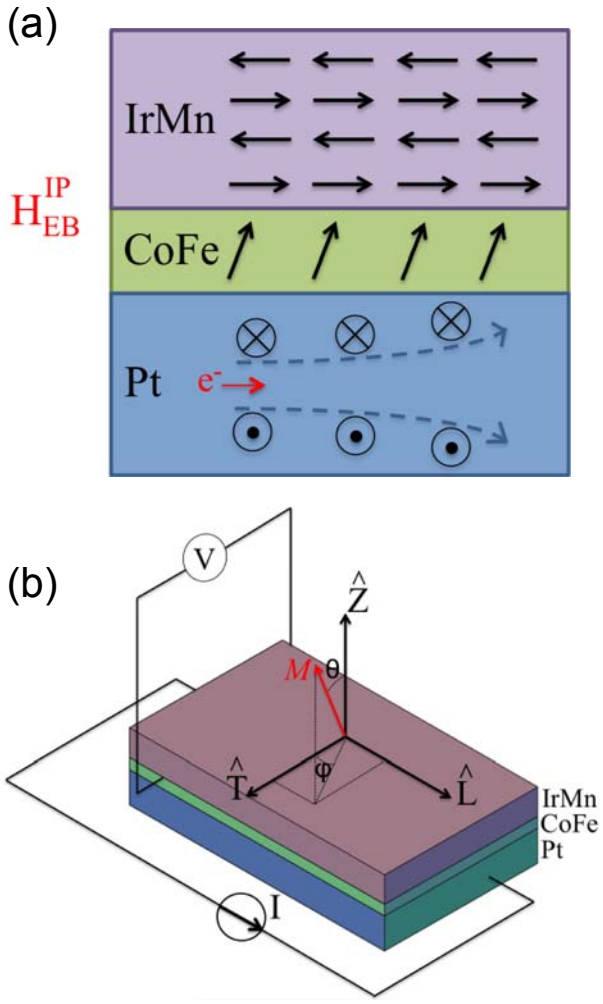

FIG. 1. (a) The studied structure for field-free switching. An antiferromagnet is placed on top of the ferromagnetic layer with perpendicular magnetic anisotropy. A spin current is generated in Pt, and exerts torques on the magnetization of the ferromagnetic layer. The in-plane exchange bias, H_{EB}^{IP}, replaces the external field for field-free switching. (b) Schematic of the measurement. I and V show the applied current direction, and the measured voltage, respectively. The direction of the exchange bias field is either out-of-plane, along $\hat{Z}$, or in the longitudinal direction, $\hat{L}$. For all the measurements a Hall bar was used. For current-driven switching measurements an external magnetic field was applied along the current direction, $\hat{L}$. Hall voltage was induced by a current I of constant amplitude 0.5 mA, which was then converted to Hall resistance. M is the magnetization direction, and θ and φ are its polar and azimuthal angles.

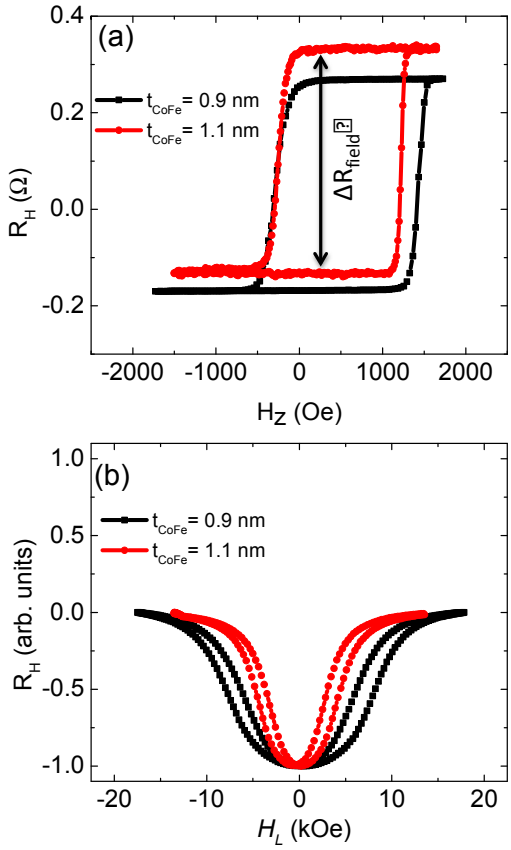

FIG. 2. (a) Perpendicular magnetic anisotropy and out-of-plane exchange bias in samples with $t_{CoFe} = 0.9$ and 1.1 nm, measured by anomalous Hall resistance. The samples are annealed with magnetic field in the $-Z$-direction. (b) Anomalous Hall resistance measured with an in-plane field, H_L. The small hysteresis loops are due to slight misalignments between the field and the surface of the samples.

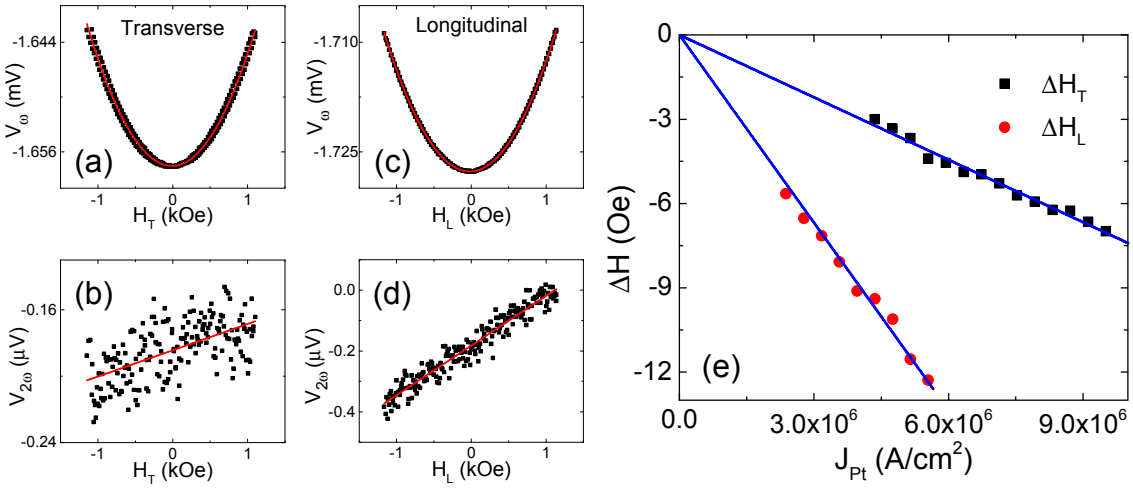

Fig. 3. First and second harmonic anomalous Hall voltages for the field-like field measurement (a)-(b) and damping-like field measurement (c)-(d). H_L and H_T represent the fields applied along current (longitudinal) and voltage (transverse) channels, respectively. The applied current has an amplitude of 7mA. (e) Field-like and damping-like fields dependence on the peak current density of Pt. The solid line represents the best linear fitting result, with zero intercept.

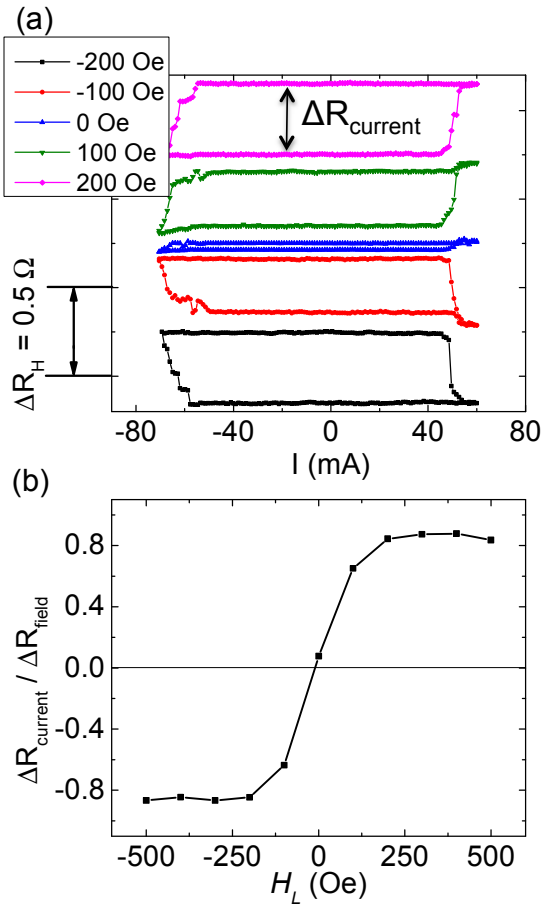

FIG. 4. (a) Current driven switching in the sample with out-of-plane EB, in the presence of different external in-plane magnetic fields, H_L. No asymmetry in $|\Delta R_{current}|$ between positive and negative magnetic field values is observed. A current of 45 mA corresponds to a current density of $\sim 4 \times 10^7$ A/cm^2, passing through the Pt layer. (b) The switching diagram. No shift, or equivalently no field-free switching, is observed. Positive and negative values correspond to different switching polarities. For this sample $\Delta R_{field} = 0.473\ \Omega$.

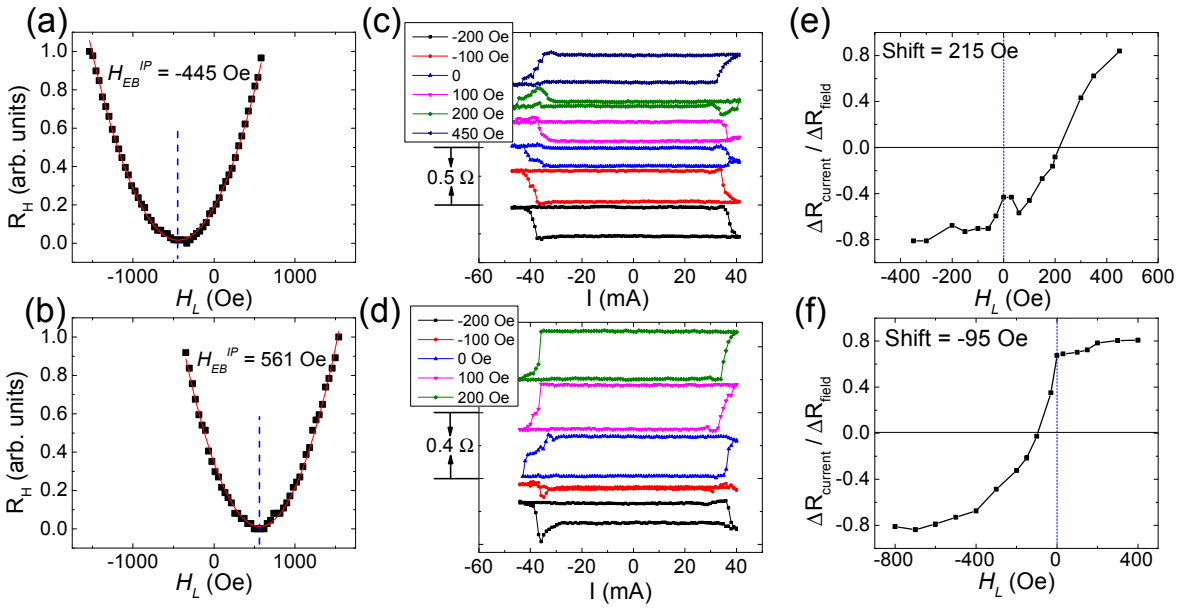

FIG. 5. (a), (b) In-plane exchange bias field introduction, in two different directions. The red line is the quadratic fit; the resulting extremum yields the in-plane exchange bias field. (c), (d) Current driven switching with in-plane exchange bias in two different directions, measured at different values of applied in-plane field H_L. $|\Delta R_{current}|$ is, in each case, asymmetric with respect to different fields. Field-free switching is observed. A current of 35 mA corresponds to a current density of $\sim 3.1 \times 10^7$ A/cm^2, passing through the Pt layer. (e), (f) The switching diagram for different in-plane exchange bias directions. Shifts to opposite directions is observed, which is consistent with the exchange bias field directions. It should be noted that (a), (c), (e) are the results for first direction, and (b), (d), (f) are the results for the second one.

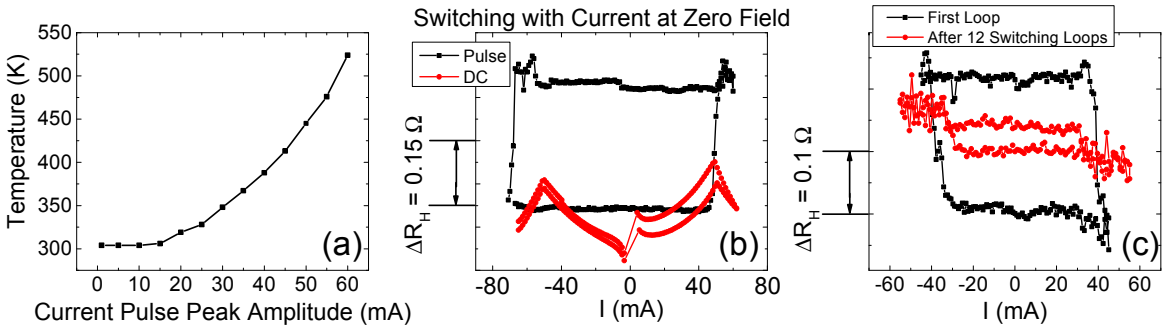

FIG. 6. (a) Temperature change at different current pulse peak amplitudes. (b) Current driven field-free switching comparison of DC and pulsed currents. With pulse current, field-free switching is achieved, while with DC almost no change in the Hall resistance is observed. This is attributed to Joule heating effect. (c) The degrading of field-free switching after 12 successive switching measurements. For this purpose only pulsed current has been used, and the same measurement has been repeated 12 times. A current of 35 mA corresponds to a current density of $\sim 3.1 \times 10^7$ A/cm^2, passing through the Pt layer.

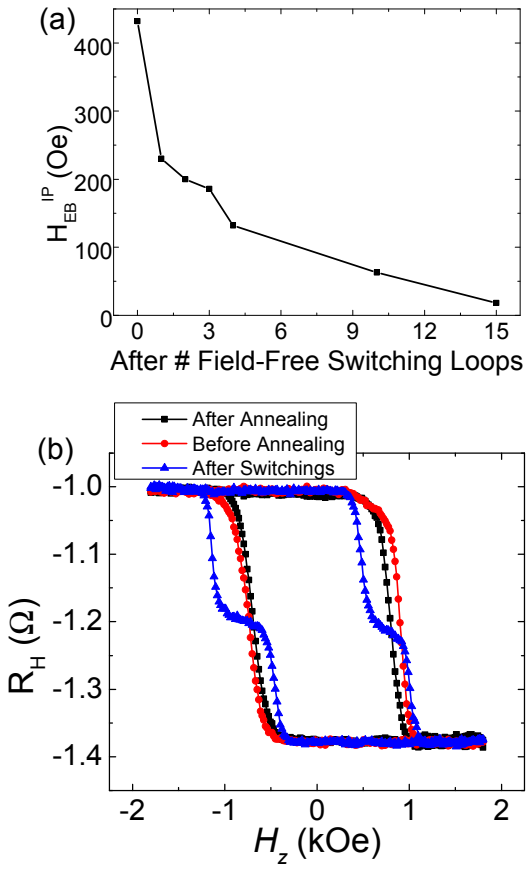

FIG. 7. (a) In-plane exchange bias change after several field-free current-driven switching cycles. A current of 0.1 mA was used for the exchange bias measurement. (b) Anomalous Hall measurement with out-of-plane field, before and after current annealing with in-plane field, and after current-driven switching measurement. Annealing in the presence of in-plane field reduces the out-of-plane exchange bias. After switching measurement, the out-of-plane exchange bias appears again, in the form of double loops.

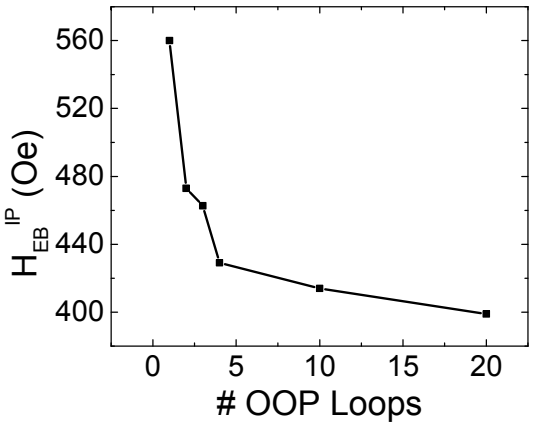

FIG. 8. Training effect of the in-plane exchange bias, after successive switching cycles with an out-of-plane field. After each out-of-plane loop, the in-plane exchange bias field is decreased, but it has a saturation value. A current of 0.1 mA was used for the measurements.